Mathematical Modeling and Evaluation of Performance Characteristics of a Hybrid Solar PV and Wind Energy System

Kiran Kumar B M[1*], M S Indira[1], and S Nagaraja Rao[1]

[1] M S Ramaiah University of Applied Sciences, Bangalore, India
[*] Corresponding author. E-mail: kirankumar.ee.et@msruas.ac.in

Received: May 16, 2021; Accepted: July 23, 2021

Solar Photovoltaic (SPV) and wind energy are two major sources of renewable energy that are intermittent in nature. A hybrid system consisting of SPV and Wind Energy Conversion System (WECS) can meet the energy needs as either of the source continues to generate energy, in the absence of the other that is reliable and cost effective. The paper presents detailed mathematical modelling, simulation and performance analysis of a single cell SPV and Permanent Magnet Synchronous Generator (PMSG) based WECS. These two sources are integrated to form a hybrid renewable energy system. The hybrid model is simulated and the overall performance is analyzed using MATLAB/Simulink for varying temperature/irradiation conditions and varying wind speeds for SPV and WECS respectively. Performance characteristics of the hybrid PV and WECS are presented. The paper also presents as a case study, the annual energy generation for a chosen location from individual SPV and WECS systems based on the real time data collected from Solacast website. This study evaluates the feasibility of implementation of a hybrid system at the site.

Keywords: Boost converter, Irradiation, Solar Photovoltaic, Temperature, Wind speed

http://dx.doi.org/10.6180/jase.202208_25(4).0014

1. Introduction

Rapid depletion of fossil fuel and growing environmental concerns have led to the decline of using conventional energy sources to meet world's energy demand. Thus switching to alternative energy source like solar, wind, tidal, etc that are renewable in nature became a necessity. Renewable Energy Sources (RES) play a key role in production of clean, green energy. As per International Energy Agency (IEA), the share of RES in worldwide energy generation has increased to 28% in the year 2020 from 26% in 2019. In recent years, SPV and WECS are considered to be the most popular of all available RES [1–4]. The reason being evident as the sources are available freely in nature, are inexhaustible with lower maintenance costs and reduced carbon foot prints. [2, 5]. Advancement in power converter technology has also led to reduction in energy generation costs [1].

World, in the recent past has witnessed an increasing trend in research and development in the associated areas like the material used in construction of the solar cells and wind turbine, aerodynamics of rotor blades; system design; improvement in their performance characteristics etc. Globally there has been a huge deployment of both solar PV and WECS off late. The annual growth rate of the solar PV industry is approximately 35-40 per cent and is one of the fastest-growing industries [6, 7] . It is also expected to have a 25% share of total electricity generation from solar PV by 2050 [7]. Similarly, technological advancement in wind turbine aerodynamics and micrometeorology contribute to a rise in the energy yield in wind turbines of about 5% annually [8].

According to the European Council for Renewable Energy, RES will contribute about 50% of the global energy demand by 2040 [9]. A block diagrams of typical solar PV

and WECS system connected to suitable power converters are depicted in Fig. 1 (a) and Fig. 1 (b) respectively.

The performance of both SPV and WECS rely primarily on environmental factors i.e., irradiation/ temperature and wind speed respectively. The output of SPV and WECS cannot be accurately predicted as the availability of these quantities are highly intermittent and sporadic in nature and hence it is not preferred to use either SPV or WECS to generate electric power unless their availability is ensured for 80-90% of the duration annually.

Therefore, a hybrid RES with a combination of solar/wind, solar/hydro, wind/hydro or a combination of all three would be viable proposition for continuous generation of energy. Hybrid RES have been studied by various researchers [10–14]. A hybrid solar PV and WECS is found to be more reliable as the system is complimentary in nature, commercially viable with reduced size of the Battery Storage System (BES) [10]. The hybrid system can be used for off grid or on grid applications with or without a storage system. A typical hybrid solar PV and WECS is depicted in Fig. 2.

A detailed mathematical model of a SPV and WECS is presented with simulation results for their output performance under varying temperature, irradiation and wind speeds respectively. SPV and WECS are integrated to form a hybrid system with suitable power converters. Performance characteristics and output of the hybrid PV and WECS are evaluated.

2. Mathematical Modelling of Solar PV

The output of SPV system being nonlinear, primarily depends on irradiation and temperature. It also depends on other physical parameters such as, series and shunt resistance, number of series and parallel cells, density of accumulated dust on the SPV panel, partial shade, and so on. The solar PV module output thus varies with irradiation, temperature and other physical parameters. The efficiency of current solar cell technology is reported to be more than 25% [15].

Tracking the point of maximum power generation in a SPV system is critical and several techniques are available [16–21]. An appropriate Maximum Power Point Tracking (MPPT) technique is usually used to extract the maximum possible power from the PV panel. The present work is limited to modelling and simulation of PV system. Mathematical model of solar PV is developed based on its electrical equivalent circuit. An ideal PV cell consists of a single current source coupled in parallel to a diode.

while, the practical model is indicated with shunt and series resistances on the output side. Physical effects of the p-n junction is represented by the diode while the current source indicates photo current. An electrical equivalent circuit of solar PV is depicted in Fig. 3 and the two important parameters associated are short circuit current (I_{sc}) and open circuit voltage (V_{oc}).

The SPV output current is proportional to the irradiation and its output voltage is inversely proportional to the temperature.

The output current of the SPV model is shown in Fig. 3 is given as

$$I = I_{ph} - I_D - I_{sh} \tag{1}$$

Here, I_{ph}: SPV current (A), I_D: Current through diode (A), I_{sh}:Current through shunt resistor R_{sh} (A).

SPV current is given by

$$I_{ph} = [I_{sc} + K_i(T - 298)]\,\frac{G}{1000} \tag{2}$$

Where, I_{sc} = Short Circuit (SC) current (A), K_i = Co-efficient of short circuit current of PV cell at standard test conditions (T= 25°C and G =1000 W/m^2), T = Operating temperature (°C), G = Solar Irradiation (W/m^2).

Diode current is given by

$$I_D = I_o\left[e^{\frac{q\left(V+IR_S\right)}{nkTN_S}} - 1\right] \tag{3}$$

Where, q = Electric charge = 1.6×10^{-19} (C), n = Diode ideality factor = 1.3, R_s = Series resistance (Ω), k = Boltzmann constant = 1.38×10^{-23} J/K, N_s=Cells in series, $I_\circ$: Diode saturation current and given by

$$I_o = I_{rs}\left(\frac{T}{T_n}\right)^3 \cdot e\left[\frac{qEgo\left(\frac{1}{T_n} - \frac{1}{T}\right)}{nk}\right] \tag{4}$$

Here, T_n = Nominal Temperature = 298(°K), E_{go}=Band gap energy of the semiconductor (eV) = 1.1eV, I_{rs}:Cell reverse saturation current given by.

$$I_{rs} = \frac{I_{Sc}}{\left[e^{\left(\frac{qV_{Oc}}{nkTN_S}\right)} - 1\right]} \tag{5}$$

Finally, Shunt current of the PV model is given by

$$I_{sh} = \frac{V + IR_{sh}}{R_{sh}} \tag{6}$$

From Eq. (5) and Equation Eq. (6): V_{oc}=Open circuit voltage (V), R_{sh}=Parallel/Shunt resistance (Ω).

The SPV is simulated in MATLAB/Simulink, based on the standard characteristics of PV cell defined by the manufacturer and shown in Fig. 4. Hence, the model is developed based on the data given in the Table 1

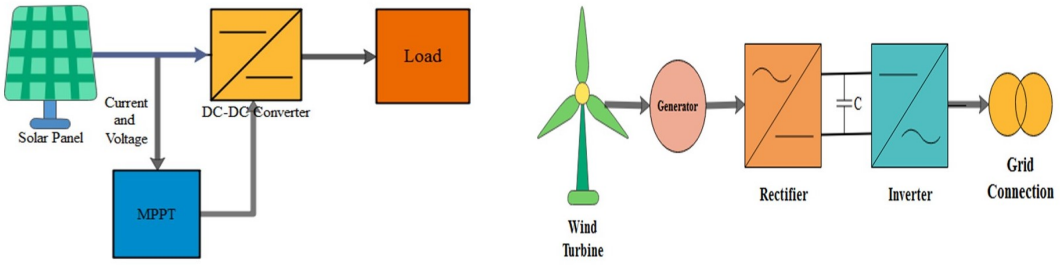

(a) (b)

Fig. 1. Block Diagram of (a) SPV (b) WECS

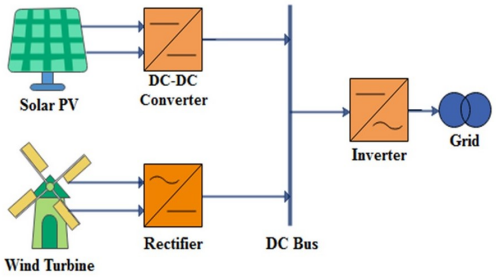

Fig. 2. A typical hybrid SPV and WECS

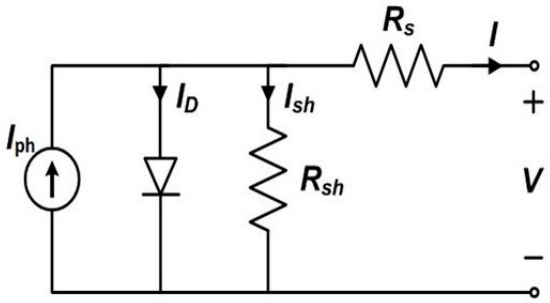

Fig. 3. Equivalent circuit of SPV

The P-V curve for changing T and G are depicted in Fig. 5 (a) and Fig. 5 (b) respectively. The I-V curve for changing T and G are depicted in Fig. 6 (a) and Fig. 6 (b) respectively. The output of SPV is connected to DC-DC converter to increase the output voltage to 100 V DC and the output waveform is shown in Fig. 7.

The output characteristics of SPV clearly shows that the output voltage is inversely proportional to the T and the output voltage decreases as T increases and the power generated reduces. Also, it can be noted that the output current is directly proportional to the irradiation hence, current increases with irradiation. The output voltage and power for various temperature and output current and

Table 1. Electrical Parameters of ASP4FC200 Apollo solar cell.

Solar cell Parameters	Values
Maximum Power (P_{max})	200 W
V at P_{max}	26.7 V
I at P_{max}	7.5 A
Voc	32.6 V
Isc	8.3 A
K_i (Temperature coefficient)	4.46 (mA/K)
K_v (Temperature coefficient)	-2.13 (mV/K)
Temperature coefficient of P_{max}	-0.44 (%/°C)
Operating Cell Temperature (NOCT)	298 K
Cells in parallel	Single cell
N_s	54

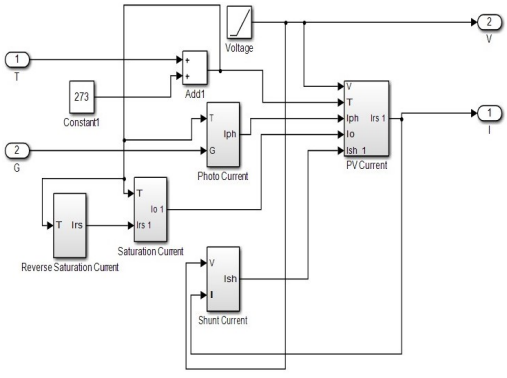

Fig. 4. MATLAB/SIMILINK model of Solar PV

Table 2. Output voltage and power for different temperature.

Temperature (C)	Voc (V)	Pm(W)
10°	39.5	256.19
15°	38.5	248
20°	37.4	239.7
25°	36.4	231.4
30°	35.5	223.2
35°	34.4	215

Table 3. Output current and power for different Irradiation values.

Irradiation W/m^2	Isc (A))	Pm(W)
250	2.06	55.82
500	4.12	115.2
750	6.17	173.6
1000	8.22	230.4
1250	10.27	288.6
1500	12.32	344.7

power for various irradiation are tabulated in Table 2 and Table 3 respectively.

3. Mathematical Modelling of Wind Turbine (WT)

3.1. Modeling of WT

WECS integrates three important building blocks: WT, drive train and generator. The direct drive PMSG based WECS consists of: WT, generator, rectifier and control unit. A typical direct drive PMSG based WECS is shown in Fig. 8.

This paper presents a mathematical model of a horizontal axis WT and its output is characteristics. The simulation results for various input parameters: wind velocity and pitch angle are presented.

The blades of WT extract the wind's Kinetic Energy (KE) and convert it into mechanical energy. The KE of an object with mass m in air with velocity v is given as

$$E = \frac{1}{2}mv^2 \tag{7}$$

The moving air power (assuming constant speed) is given by

$$P_w = \frac{dE}{dt} \tag{8}$$

Substituting the value of 'E' from Eq. (8)

$$P_w = \frac{1}{2}\frac{dm}{dt}v_w^2 \tag{9}$$

Where $\frac{dm}{dt}$ is rate of mass flow= $\rho A v_w$.

The power in the air can be represented as when the air passes over Area 'A'

$$P_w = \frac{1}{2}\rho A v_w^3 \tag{10}$$

Where 'ρ'is air density and given by ρ = 1.225 kg/m^3, A= Area swept by turbine blades in m^2, v_w=Speed of wind in m/s.

Therefore, the mechanical power of wind turbine is given by

$$P_m = \frac{1}{2}AC_p(\lambda,\beta)v_w \tag{11}$$

Where, C_p (λ,β) = Power coefficient (Maximum value = 0.593), usually a function of two parameters: λ;Tip speed ratio; β;Blade pitch angle in degrees.

Tip speed ratio of WT blade is given by:

$$\lambda = \frac{\omega_m R}{v_w} \tag{12}$$

Where, ω_m = Rotor angular velocity (rad/s), R= Rotor radius (blade length) (m).

The power coefficient (C_p) of WT is given by:

$$C_p(\lambda,\beta) = C_1\left(\frac{C_2}{\lambda_i} - C_3\beta - C_4\right)e^{\frac{-c_5}{\lambda_i}} + C_6\lambda \tag{13}$$

Where, The coefficients; C_1= 05176, C_2=116, C_3=0.4,C_5=21 and C_6=0.0068 The maximum value of 'C_p' is 0.48 is achieved at pitch angle β=0 and λ=8.1 and considered as nominal value shown in Fig. 11 (a).

$$\lambda_i = \frac{1}{\left(\frac{1}{\lambda+0.089\beta} - \frac{1}{\beta^3+1}\right)} \tag{14}$$

Hence, the rotor aerodynamic torque T_w is given by:

$$T_w = \frac{P_m}{\omega_m} \tag{15}$$

Substituting for 'P_m' in Eq. (15)

$$T_w = \frac{\frac{1}{2}C_p(\lambda,\beta)\rho A v^3}{\omega_m} \tag{16}$$

Where, A= Area covered by the blades and represented by:

$$A = \pi R^2 \tag{17}$$

Substituting for 'A' in Eq. (16)

$$T_w = \frac{\frac{1}{2}\pi C_p(\lambda,\beta)\rho R^2 v^3}{\omega_m} \tag{18}$$

The WT simulated in MATLAB/Simulink environment shown in Fig. 9 is based on the standard specifications of WT given is Table 4. A typical WT power curve is shown in Fig. 10 that represents the power generated (kW) by WT at different wind speeds (m/s).

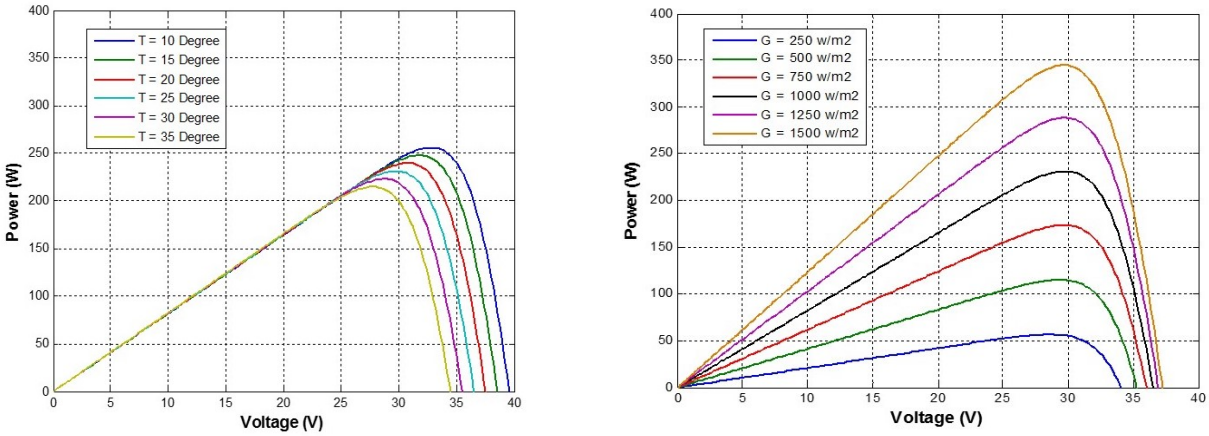

(a) P-V curve for changing T values. (b) P-V curve for changing G values

Fig. 5. (a) I-V curve for varying temperature values. (b) I-V curve for varying irradiation values

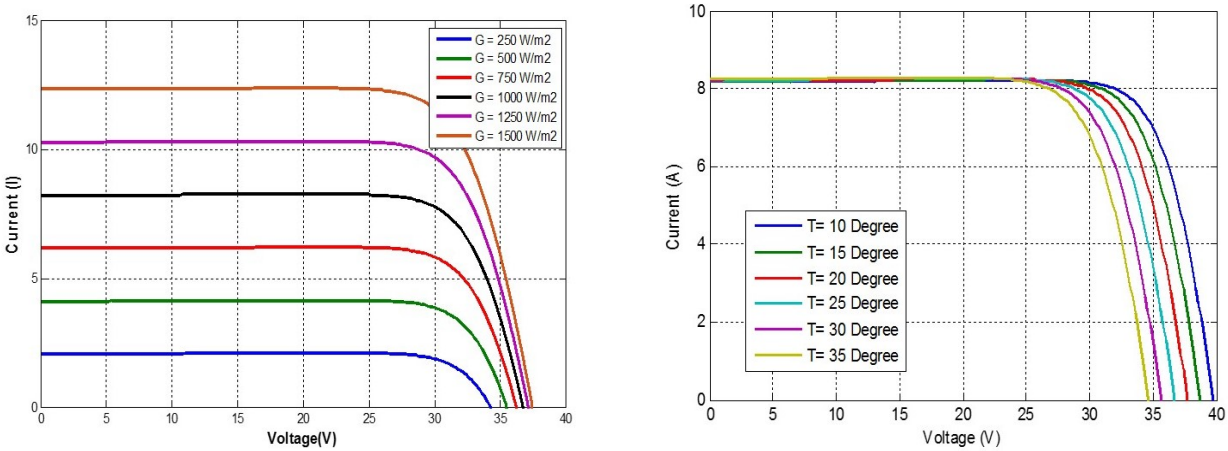

(a) P-V curve for changing T values. (b) P-V curve for changing G values

Fig. 6. (a) I-V curve for varying temperature values. (b) I-V curve for varying irradiation values

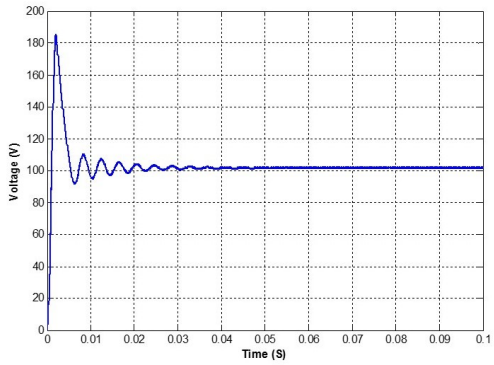

Fig. 7. Output voltage of SPV with DC-DC converter

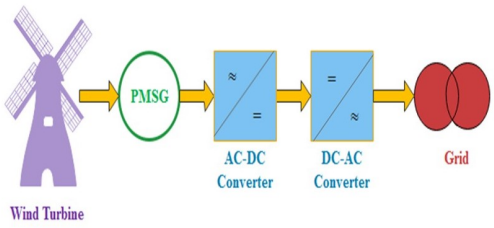

Fig. 8. A typical direct drive PMSG based WECS

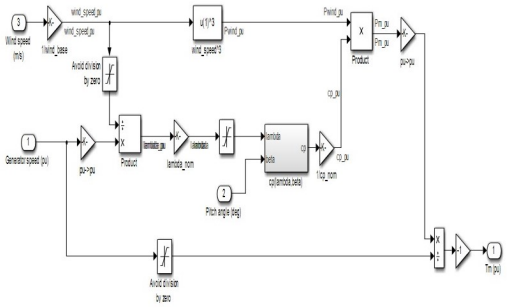

Fig. 9. Simulation model of WT in MATLAB

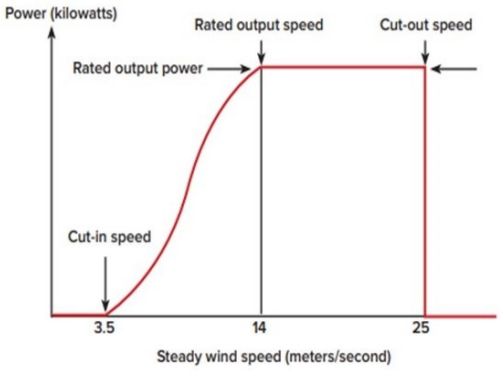

Fig. 10. Typical Wind Turbine Power Curves

Also, C_p vs λ characteristics, for various values of β and turbine power characteristics with respect to pitch angle β that represents output power in per unit value with respect to turbine speed is depicted in Fig. 11 (a) and Fig. 11 (b) respectively.

3.2. Modeling of PMSG

Wind turbines are broadly classified as horizontal axis and vertical axis WT. Various types of generators have been used in WECS [22, 23]. PMSG, doubly fed induction generators, synchronous generators and induction generators are commonly used these days. Permanent magnet synchronous generator has many advantages like; reliable, high efficiency, small size and less maintenance compared to other generators [24, 25] hence, PMSG based horizontal axis wind turbine is simulated. The modeling of PMSG is done in 'dq' reference frame [26] based on DC voltages and currents.

Table 4. Specification of WT.

Parameter	Value
Mechanical output power	3 kW
Rotor Diameter	26 meters
Wind Speed	Varied
Type of Turbine	Horizontal axis WT
Air Density	1.225 kg/m^3
Blade pitch angle	0
C_p	0.48

The current equations in 'd' axis and 'q' axis are given as:

$$\frac{di_{sd}}{dt} = -\frac{R_{sa}}{L_{sd}} i_{sd} + \omega_d \frac{L_{sq}}{L_{sd}} i_{sq} - \frac{1}{L_{sd}} v_{sd} \tag{19}$$

$$\frac{di_{sq}}{dt} = -\frac{R_{sa}}{L_{sq}} i_{sq} - \omega_s \left(\frac{L_{sd}}{L_{sq}} i_{sd} + \frac{1}{L_{sq}} \Psi_p \right) + \frac{1}{L_{sq}} v_{sq} \tag{20}$$

And, the electromagnetic torque equation of the rotor is given by:

$$T_e = 1.5 \frac{P}{2} \left[\Psi_p i_{sq} + i_{sd} i_{sq} \left(L_{sd} - L_{sq} \right) \right] \tag{21}$$

Where; R_{sa} is resistance of stator
v_{sd} and v_{sq}; d_q axis stator voltages
i_{sd} and i_{sq}; d_q axis stator currents ω_s Angular velocity of the generator L_{sd} and L_{sq} are the inductance of the generator Ψ_p is the permanent flux

The Simulink model of WECS is shown in Fig. 12. Mechanical torque developed at the output of WT is directly

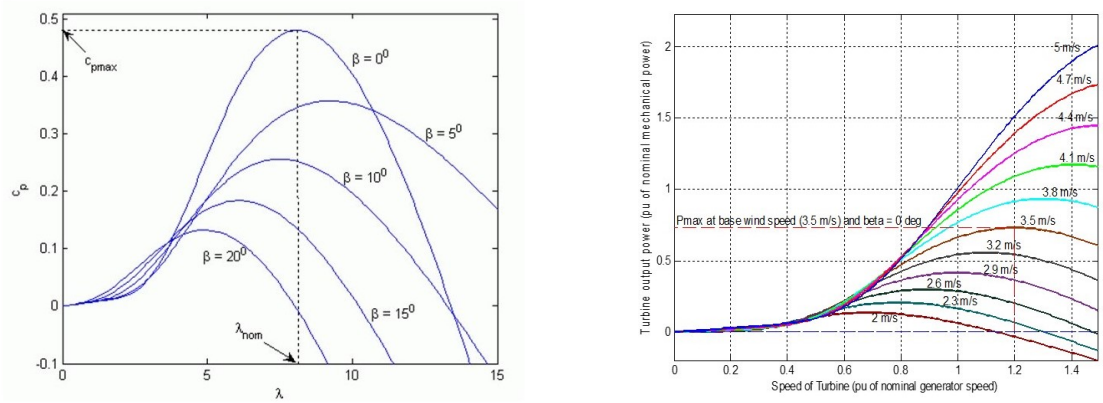

(a) (b)

Fig. 11. (a) Cp vs λ characteristics, for various values of β. (b). Power Characteristics of Turbine (β = 0 degree)

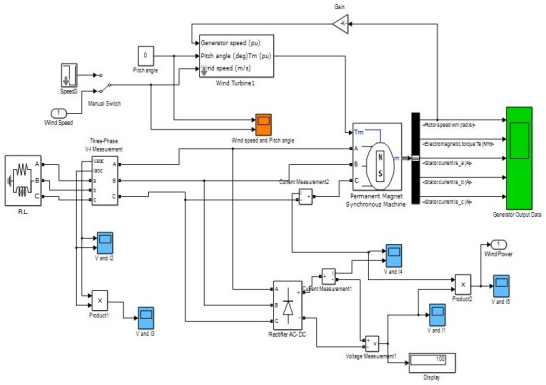

Fig. 12. MATLAB/Simulink model of PMSG based WECS

Table 5. Output of WECS for various wind speeds.

Wind Speed (m/s)	Output Voltage (V)	Power Output (W)
3.5	62.19	385
4.0	72.28	524.4
4.5	82.21	675.4
5.0	91.82	841.5
5.5	101.2	1029
6.0	110.3	1221
6.5	119	1412
7.0	127.4	1613
7.5	135.3	1820

fed to PMSG as input. Rotor speed of PMSG is fed back to the WT, β of the WT is maintained at '0' to get maximum power coefficient (C_p) from WT. Base speed of WT is set to 3.5 m/s.

The AC voltage is developed at output of the PMSG is rectified using bridge rectifier. The simulation is done at 5.5 m/s wind velocity to maintain the output voltage of WECS at 100 V DC to connect in parallel with solar PV. The output DC voltage waveform is depicted in Fig. 13 (a) and output power is 1024 W, as depicted in Fig. 13 (b). The output voltage is directly proportional to wind speed. The output of WECS for various wind speed is tabulated in Table 5.

4. Hybrid PV and WECS

The solar irradiation and wind speed being intermittent in nature, integration of these two sources would result in a highly efficient and reliable system as they would complement each other ensuring continuity in supply [27]. This has made the hybrid PV and WECS more popular off late. The hybrid system with two sources operating in parallel connected to a load (DC) is depicted in Fig. 14 and the Simulink model in Fig. 15. The output of WECS is adjusted to generate 100 V DC. The output of solar PV being 50 V DC is connected to a simple conventional DC-DC converter to boost the output to a required level of 100V to match the WECS output.

The output of hybrid system is measured at standard test conditions of 1000 W/m^2 irradiation of 25° C temperature for SPV. According to National Institute of Wind Energy, the average wind speed at Peenya, Bangalore is 4-5 m/s at 20 meter height but a wind speed of 5.5 m/s is considered for simulation. The system is simulated and the output of Hybrid PV and WECS has a first peak overshoot of about 20 % of output voltage as depicted in Fig. 16 (a). The oscillations in the output voltage, current and power are minimized by connecting a suitable value of series inductor (L) on the source side with filter capacitor on load

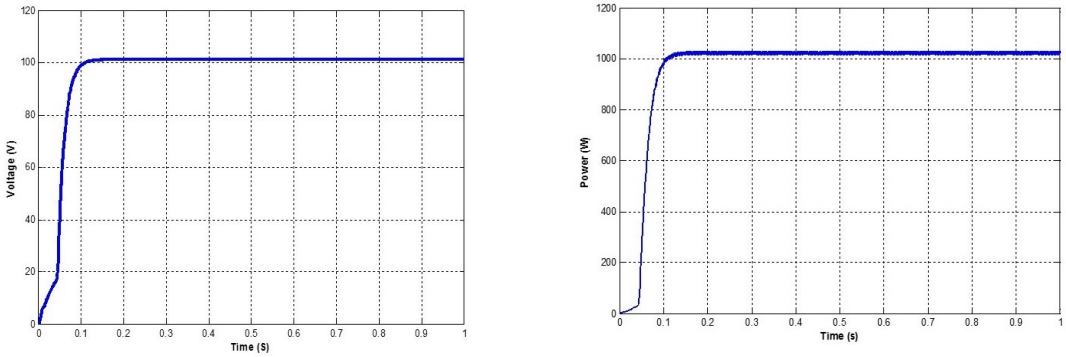

(a) (b)

Fig. 13. (a). DC output voltage of WECS. (b). DC output power of WECS

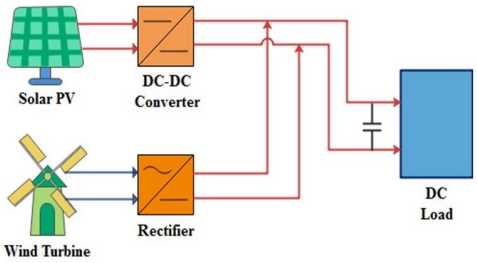

Fig. 14. Block diagram of Hybrid PV and WECS

side. This results in reduction of peak overshoot from 20 % to 17 % in output voltage and current, from 45 % to 40 % in output power.

The DC output voltage across the load is 98 V is shown in Fig. 16 (b) and a current of 9.79 A through the load is depicted in the Fig. 17 (a). The power output of the hybrid PV and WECS is 960 watts as shown in Fig. 17 (b). The hybrid PV and WECS can be further connected to an inverter to be integrated with the grid.

5. Case Study

The developed mathematical models are used to establish the feasibility of implementing a hybrid system at a chosen location. Based on the hourly measured meteorology data from Solcast website, the monthly average data of solar irradiation, temperature and wind speed over a year at a 20 meter height can be forecasted. The data has been measured for the location Peenya, Bangalore, Karnataka, India (Latitude: 13°.0183″ and Longitude: 77°.5082″).

The data has been considered for a year starting from October 2019 to September 2020. Fig. 18 illustrates the monthly average solar irradiation at the chosen location from 9AM to 5PM. Fig. 19 illustrates the monthly average temperature from 9AM to 5PM .The average annual solar irradiation and temperature is 529 W/m^2 and 27.50°C respectively. Fig. 20 illustrates the average monthly wind speed in the chosen location at 20 meter height and the average annual of wind speed is 4.15 m/s.

The above data from Solcast is used to predict the average annual individual power generation from SPV and WECS for a particular location. The real time data such as solar irradiation, atmospheric temperature and speed of the wind are used as inputs for the developed model of SPV and WECS systems and the simulation results obtained for hourly average power generated is shown in Fig. 21. Also, the simulation results for monthly average energy generated by SPV and WECS are tabulated in Table 6 and Table 7 respectively.

The sun light in a day may available for nine to ten hours a day but, peak sun hours to calculate the amount of power generated by SPV is considered as four hours per day. The hourly average of solar irradiation over a year is noted and daily average solar irradiation is calculated for four hours (peak sun hours). Hence the average daily energy generation from SPV according to the data collected for the month March 2019 is 179×4 = 716 Wh. For the entire month the energy generated from SPV alone will be 22.196 kWh.

Similarly, the average daily energy generation considering 25 percent capacity factor for WECS from the data collected for the month of March is 349×24×0.25 = 2.09kWh. Hence, for the month of March 2019 the energy generated from WECS is 2.09×31 = 64.9 kWh. The total average monthly energy generation from SPV and WECS for the duration October 2019 to September 2020 is shown in the

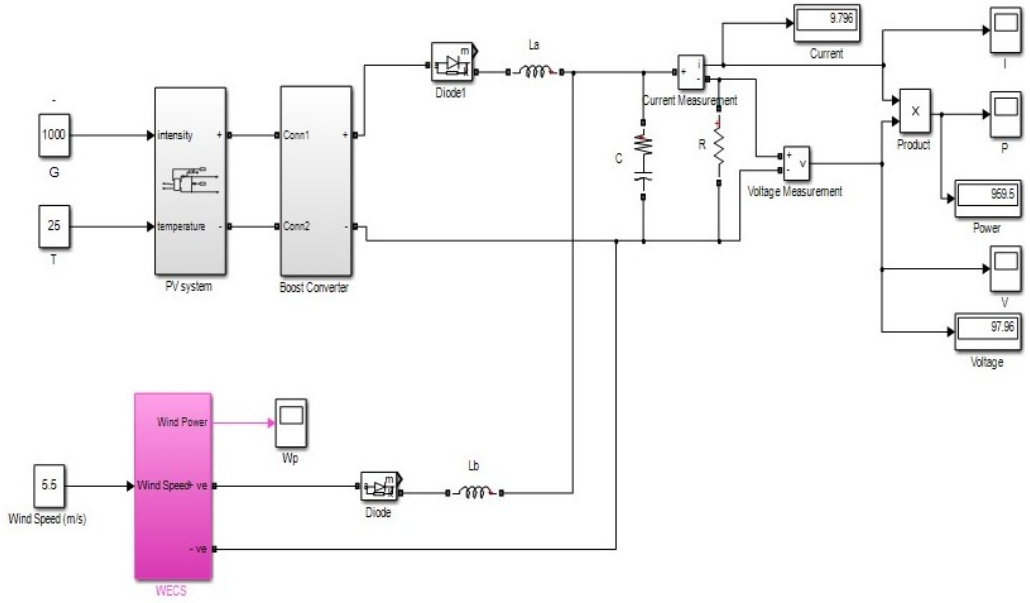

Fig. 15. MATLAB/Simulink model of Hybrid PV and WECS

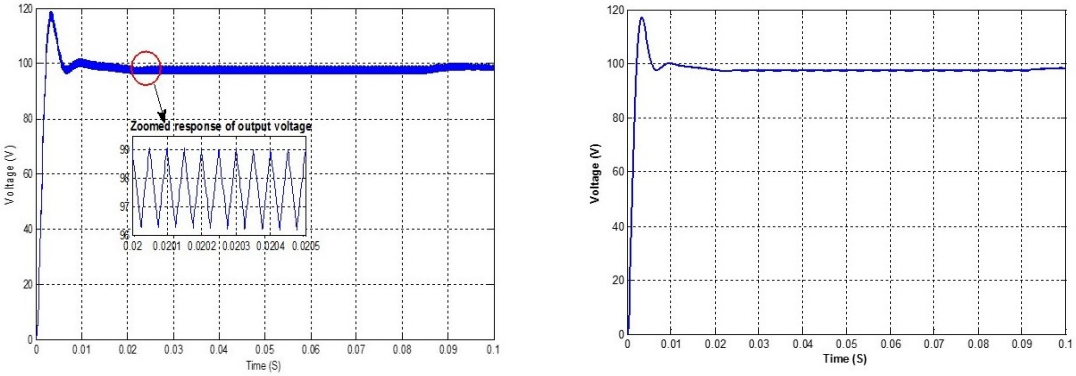

(a) (b)

Fig. 16. (a). Output voltage of hybrid SPV and WECS without series L. (b). DC output voltage of hybrid SPV and WECS with series L

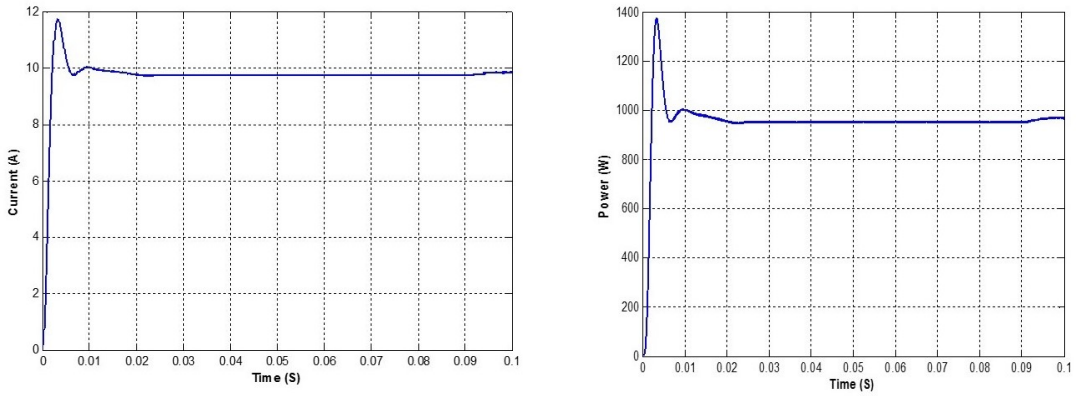

(a) (b)

Fig. 17. (a). DC output current of hybrid SPV and WECS with series L.
(b). DC output power of hybrid SPV and WECS with series L

Table 6. Monthly average energy generated by SPV system.

Month	**Irradiation** (W/m^2)	**Temperature** (C)	**Hourly average power output** (Watts)	**Energy generated** (kWh)
October	350	25.8	92	11.4
November	486	25.7	128	15.3
December	460	23.8	122	15.1
January	637	26.1	167	20.7
February	696	27.5	180	20.8
March	698	30.1	179	22.1
April	690	32.4	174	20.8
May	627	32.7	157	19.4
June	461	27.8	118	14.1
July	450	26.5	116	14.3
August	430	26.4	113	14.0
September	368	25.8	97	11.6

Table 7. Monthly average energy generated by WECS system.

Month	**Wind Speed** (m/s)	**Hourly average power output** (Watts)	**Energy generated** (kWh)
October	3.4	361	67.1
November	3.8	465	82.0
December	4.31	615	114.3
January	3.56	402	74.7
February	3.72	444	77.2
March	3.35	349	64.9
April	3.5	386	69.4
May	3.56	402	74.7
June	5.3	951	171.1
July	4.77	764	142.1
August	6.2	1295	240.8
September	4.9	840	151.1

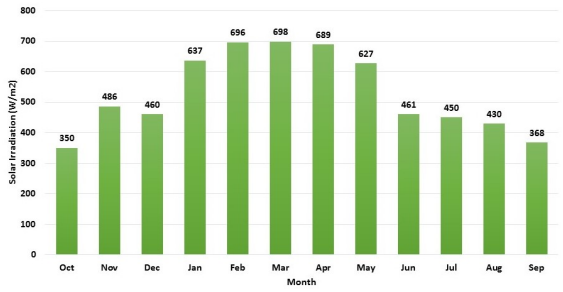

Fig. 18. Monthly average solar irradiation from October 2019 to September 2020 at Peenya Bangalore

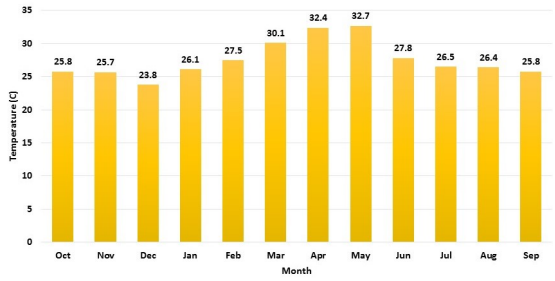

Fig. 19. Monthly average temperature from October 2019 to September 2020 at Peenya Bangalore

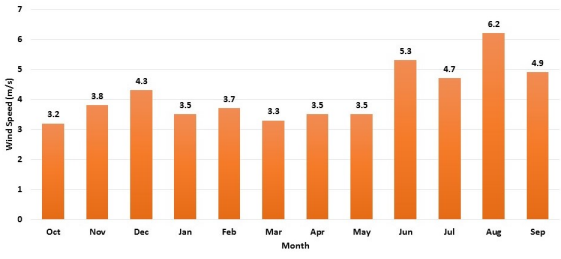

Fig. 20. Monthly average wind speed from October 2019 to September 2020 at Peenya Bangalore

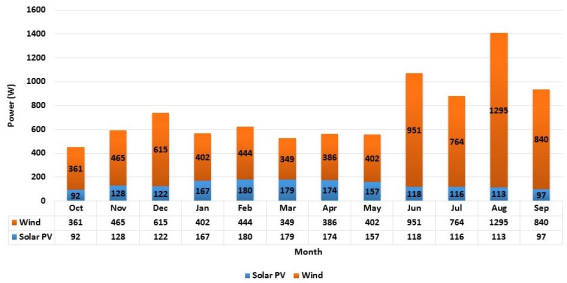

Fig. 21. Hourly average power generation from SPV and WECS from October 2019 to September 2020 at Peenya Bangalore

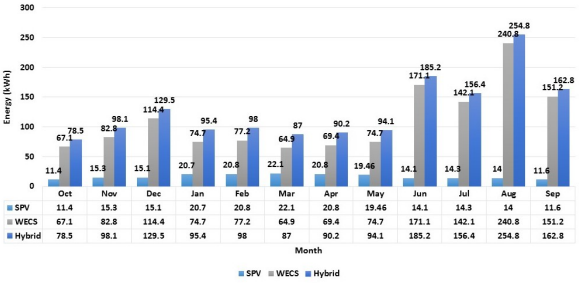

Fig. 22. Average monthly and cumulative energy generation from SPV and WECS

Fig. 22.

The cumulative average monthly energy generation from both SPV and WECS is calculated and the results are tabulated in Table 8. Total annual energy generated by SPV alone is 199.66 kWh and WECS alone is 1330.4 kWh. An effective integration or hybridization of SPV and WECS would generate an annual energy of 1530 kWh that would be sufficient to power up a one Bed Room Kitchen (BHK) residential unit.

6. Conclusion

A detailed mathematical model of a single cell SPV is presented with relevant characteristic equations that are developed based on electrical equivalent circuit. The output characteristics of SPV are obtained for various irradiance and temperature conditions and the results are tabulated. A detailed mathematical model of direct drive PMSG based WECS is also developed and output characteristics are obtained for various input parameters; wind speed and pitch angle using simulation results.

The C_p vs λ characteristics for various values of β has been simulated. Also, the simulation results for turbine output power for varying wind speed is presented and the

Table 8. Monthly cumulative energy generation of SPV and WECS system.

Month	SPV (kWh)	WECS (kWh)	Cumulative energy (kWh)
October	11.4	67.1	78.5
November	15.3	82.8	98.1
December	15.1	114.4	129.5
January	20.7	74.7	95.4
February	20.8	77.2	98
March	22.1	64.9	87
April	20.8	69.4	90.2
May	19.46	74.7	94.1
June	14.1	171.1	185.2
July	14.3	142.1	156.4
August	14	240.8	254.8
September	11.6	151.2	162.8

output power developed are tabulated. A hybrid model is developed by integration of the two sources and the corresponding results are presented. The hybrid system enables a steady supply of power at the output though individually they suffer from intermittent existence of favorable conditions to generate power continuously.

Appropriate value of series inductor on the source side and filter capacitor on the load side minimize the peak overshoot and oscillations in the output voltage current and power waveforms. The simulation results shows that the output voltage of hybrid PV and wind system is 98 V DC with a current of 9.78 A and the power being 960 watts. Data obtained from Solcast website is used as inputs for simulation studies of SPV and WECS for chosen location in Peenya, Bangalore. The simulation results show the individually generated energy by SPV and WECS. The cumulative energy generated by both SPV and WECS is also presented. The annual energy of 1536 kWh generated is sufficient to power-up a single bedroom residential unit.

Acknowledgements

Authors would like to express their thanks to the VC of RUAS, Bangalore for providing all of the resources required to do this research.

References

[1] S. Lakshminarayanan, B. Kiran Kumar, S. N. Rao, and S. Pranupa, (2021) *"Current mode control of single phase grid tie inverter with anti-islanding"* **Int J Pow Elec & Dri Syst *12***(1): 241–248.

[2] A. Mahesh and K. S. Sandhu, (2015) *"Hybrid wind/photovoltaic energy system developments: Critical review and findings"* **Renewable and Sustainable Energy Reviews *52***: 1135–1147. DOI: 10.1016/j.rser.2015.08.008.

[3] M. S. Javed, A. Song, and T. Ma, (2019) *"Techno-economic assessment of a stand-alone hybrid solar-wind-battery system for a remote island using genetic algorithm"* **Energy *176***: 704–717. DOI: 10.1016/j.energy.2019.03.131.

[4] T. Shilpashree, K. B. Kumar, and S. Pranupa, (2021) *"A Comparative Study of Performance Analysis of Solar PV With Interleaved DC-DC Converters"*: 1–6. DOI: 10.1109/RTEICT52294.2021.9573809.

[5] B. K. Kumar, M. Indira, and S. N. Rao, (2021) *"Performance Evaluation of Solar PV Using Multiple Level Voltage Gain Boost Converter with CLC Cell"*: 237–251. DOI: 10.1007/978-981-16-0749-3_18.

[6] H. Patel, M. Gupta, and A. K. Bohre. "Mathematical modeling and performance analysis of MPPT based solar PV system". In: *2016 International Conference on Electrical Power and Energy Systems (ICEPES)*. IEEE. 2016, 157–162. DOI: 10.1109/ICEPES.2016.7915923.

[7] M. H. Ahmadi, M. Ghazvini, M. Sadeghzadeh, M. Alhuyi Nazari, R. Kumar, A. Naeimi, and T. Ming, (2018) *"Solar power technology for electricity generation: A critical review"* **Energy Science & Engineering *6***(5): 340–361. DOI: 10.1002/ese3.239.

[8] E. J. N. Menezes, A. M. Araújo, and N. S. B. da Silva, (2018) *"A review on wind turbine control and its associated methods"* **Journal of cleaner production *174***: 945–953. DOI: 10.1016/j.jclepro.2017.10.297.

[9] Ş. E. C. Şener, J. L. Sharp, and A. Anctil, (2018) *"Factors impacting diverging paths of renewable energy: A review"* **Renewable and Sustainable Energy Reviews *81***: 2335–2342. DOI: 10.1016/j.rser.2017.06.042.

[10] R. Naveen, P. Revankar, and S. Rajanna, (2020) *"Integration of Renewable Energy Systems for Optimal Energy Needs-a review"* **International Journal of Renewable Energy Research (IJRER)** ***10***(2): 727–742.

[11] E. Muh and F. Tabet, (2019) *"Comparative analysis of hybrid renewable energy systems for off-grid applications in Southern Cameroons"* **Renewable energy** ***135***: 41–54. DOI: 10.1016/j.renene.2018.11.105.

[12] M. D. Al-Falahi, S. Jayasinghe, and H. Enshaei, (2017) *"A review on recent size optimization methodologies for standalone solar and wind hybrid renewable energy system"* **Energy conversion and management** ***143***: 252–274. DOI: 10.1016/j.enconman.2017.04.019.

[13] S. Wagh and P. Walke, (2017) *"Review on wind-solar hybrid power system"* **International Journal of Research In Science & Engineering** ***3***(2):

[14] K. Kumar, N. R. Babu, and K. Prabhu, (2017) *"Design and analysis of an integrated Cuk-SEPIC converter with MPPT for standalone wind/PV hybrid system"* **International Journal of Renewable Energy Research (IJRER)** **7**(1): 96–106.

[15] M. Malinowski, J. I. Leon, and H. Abu-Rub, (2017) *"Solar photovoltaic and thermal energy systems: Current technology and future trends"* **Proceedings of the IEEE** ***105***(11): 2132–2146. DOI: 10 . 1109 / JPROC . 2017 . 2690343.

[16] K. Yoshikawa, W. Yoshida, T. Irie, H. Kawasaki, K. Konishi, H. Ishibashi, T. Asatani, D. Adachi, M. Kanematsu, H. Uzu, et al., (2017) *"Exceeding conversion efficiency of 26% by heterojunction interdigitated back contact solar cell with thin film Si technology"* **Solar Energy Materials and Solar Cells** ***173***: 37–42. DOI: 10.1016/j.solmat.2017.06.024.

[17] A. K. Podder, N. K. Roy, and H. R. Pota, (2019) *"MPPT methods for solar PV systems: a critical review based on tracking nature"* **IET Renewable Power Generation** ***13***(10): 1615–1632. DOI: 10.1049/iet-rpg.2018.5946.

[18] H. Abouobaida et al., (2017) *"Practical performance evaluation of maximum power point tracking algorithms in a photovoltaic system"* **International Journal of Power Electronics and Drive Systems** ***8***(4): 1744. DOI: 10.11591/ijpeds.v8i4.pp1744-1755.

[19] Y. Mahmoud. "Toward a long-term evaluation of MPPT techniques in PV systems". In: *2017 IEEE 6th International Conference on Renewable Energy Research and Applications (ICRERA)*. IEEE. 2017, 1106–1113. DOI: 10.1109/DISTRA.2017.8191226.

[20] B. Kiran Kumar, M. Indira, and S. Nagaraja Rao, (2021) *"Performance analysis of multiple gain boost converter with hybrid maximum power point tracker for solar PV connected to grid"* **Clean Energy** ***5***(4): 655–672. DOI: 10.1093/ce/zkab037.

[21] N. R. Sulake, A. K. Devarasetty Venkata, and S. B. Choppavarapu, (2018) *"FPGA implementation of a three-level boost converter-fed seven-level dc-link cascade H-bridge inverter for photovoltaic applications"* **Electronics** **7**(11): 282.

[22] A. Bensalah, M. Benhamida, G. Barakat, and Y. Amara. "Large wind turbine generators: State-of-the-art review". In: *2018 XIII International Conference on Electrical Machines (ICEM)*. IEEE. 2018, 2205–2211. DOI: 10.1109/ICELMACH.2018.8507165.

[23] A. AARIB, A. EL MOUDDEN, A. EL MOUDDEN, and A. HMIDAT, (2021) *"Control and Investigation of Operational Characteristics of Variable Speed Wind Turbines with Doubly Fed Induction Generators"* **Walailak Journal of Science and Technology (WJST)** ***18***(4): 10995–13. DOI: 10.48048/wjst.2021.10995.

[24] V. Yaramasu, A. Dekka, M. J. Durán, S. Kouro, and B. Wu, (2017) *"PMSG-based wind energy conversion systems: survey on power converters and controls"* **IET Electric Power Applications** ***11***(6): 956–968. DOI: 10.1049/iet-epa.2016.0799.

[25] T. M. Letcher. *Wind energy engineering: A handbook for onshore and offshore wind turbines*. Academic Press, 2017.

[26] Y. El Mourabit, A. Derouich, A. El Ghzizal, N. El Ouanjli, and O. Zamzoum, (2017) *"DTC-SVM Control for permanent magnet synchronous generator based variable speed wind turbine"* **International Journal of Power Electronics and Drive Systems** ***8***(4): 1732. DOI: 10.11591/ijpeds.v8i4.pp1732-1743.

[27] P. Joshi and K. Roy. "Implementation of Hybrid Wind–Solar Energy Conversion Systems". In: *Proceedings of International Conference on Data Science and Applications*. Springer. 2021, 221–240. DOI: 10.1007/978-981-15-7561-7_18.